

УДК 541.122:538.214

Magnetic Properties, EPR and NEXAFS – Spectroscopy of Iron-Doped Bi_3NbO_7 Ceramics

Nadezhda A. Zhuk^{*a}, Vladimir A. Belyy^b,
Vladimir P. Lutov^c, Boris A. Makeev^c,
Sergey V. Nekipelov^{a,d} and Lubov V. Rychkova^a

^aSyktvykar State University

55 Oktjabrskij, Syktvykar, Republic of Komi, 167001, Russia

^bInstitute of Chemistry of the Komi Science Center UB RAS
48 Pervomaiskaya Str., Syktvykar, Republic of Komi, 167982, Russia

^cInstitute of Geology of the Komi Science Center UB RAS
54 Pervomaiskaya Str., Syktvykar, Republic of Komi, 167982, Russia

^dInstitute of Physics and Mathematics
of the Komi Science Center UB RAS
4 Oplesnina Str., Syktvykar, Republic of Komi, 167982, Russia

Received 11.03.2018, received in revised form 21.05.2018, accepted 14.08.2018

The measurements of magnetic susceptibility, EPR and NEXAFS- spectroscopy study of the iron-containing solid solutions of bismuth niobate Bi_3NbO_7 has indicated that iron atoms are represented by monomeric Fe(III) and Fe(III)-O-Fe(III) exchange bound dimers with the ferromagnetic and antiferromagnetic types of exchange in the solid solutions of cubic modification. The exchange parameter and monomeric and dimeric cluster distribution in $\text{Bi}_3\text{Nb}_{1-x}\text{Fe}_x\text{O}_{7-\delta}$ depending on the content of the paramagnetic atoms were calculated according to the model of Heisenberg-Dirac-van Vleck. The solid solutions as well as iron oxides FeO, Fe_2O_3 and Fe_3O_4 were studied by the NEXAFS spectroscopy in order to determine the degrees of oxidation of iron atoms. The analysis of the NEXAFS Fe2p-spectra of iron-containing solid solutions and iron oxides revealed that the studied Fe atoms were mainly in the +3 oxidation state. The EPR spectrum of the sample with minimum iron content contained a symmetric signal with $g = 4.27$ with a weak shoulder at $g \sim 8$. The samples of $\text{Bi}_3\text{Nb}_{1-x}\text{Fe}_x\text{O}_{7-\delta}$ solid solutions at $0.02 \leq x \leq 0.04$ had a low-intensity broad band in the region of $g \sim 2.28$ of their spectra. The spectra of EPR of the solutions with $x > 0.04$ exhibited a broad, slightly asymmetric line centered around $g \sim 2.0$.

Keywords: iron, clusters, exchange interactions, EPR and NEXAFS-spectroscopy.

Магнитные свойства, ЭПР и NEXAFS – спектроскопия керамики Bi₃NbO₇, допированной атомами железа

**Н.А. Жук^а, В.А. Белый^б, В.П. Лютоев^в,
Б.А. Макеев^в, С.В. Некипелов^{а,г}, Л.В. Рычкова^а**

*^аСыктывкарский государственный университет
Россия, 167001, Республика Коми, Сыктывкар,
пр. Октябрьский, 55*

*^бИнститут химии Коми НЦ УрО РАН
Россия, 167982, Республика Коми, Сыктывкар, ул. Первомайская, 48*

*^вИнститут геологии Коми НЦ УрО РАН
Россия, 167982, Республика Коми, Сыктывкар, ул. Первомайская, 54*

*^гИнститут физики и математики Коми НЦ УрО РАН
Россия, 167982, Республика Коми, Сыктывкар, ул. Оплеснина, 4*

На основании данных магнитной восприимчивости и исследований методами ЭПР- и NEXAFS-спектроскопии железосодержащих твердых растворов ниобата висмута Bi₃NbO₇ кубической модификации установлено, что атомы железа находятся в виде мономеров Fe(III) и обменносвязанных димеров Fe(III)-O-Fe(III) с ферро- и антиферромагнитными типами обмена. По модели Гейзенберга-Дирака-ван-Флека рассчитаны обменные параметры и распределение кластеров в Bi₃Nb_{1-x}Fe_xO_{7-δ} в зависимости от содержания парамагнитных атомов. С целью определения электронного состояния атомов железа исследованы твердые растворы и оксиды железа FeO, Fe₂O₃ и Fe₃O₄ методом NEXAFS-спектроскопии. Анализ Fe2р-спектров NEXAFS железосодержащих твердых растворов и оксидов железа показал, что атомы железа имеют степень окисления +3. В ЭПР-спектре образца с минимальным содержанием железа содержится симметричный сигнал с $g = 4,27$ со слабым плечом при $g \sim 8$. В спектрах образцов твердых растворов Bi₃Nb_{1-x}Fe_xO_{7-δ} ($0,02 \leq x \leq 0,04$) содержится широкая полоса малой интенсивности в области $g \sim 2,28$. В ЭПР-спектрах растворов ($x > 0,04$) проявляется широкая, слегка асимметричная линия, центрированная вокруг $g \sim 2,0$.

Ключевые слова: железо, кластеры, обменные взаимодействия, ЭПР- и NEXAFS-спектроскопия.

Introduction

Bismuth niobate Bi₃NbO₇ and its solid solutions are perspective basic substances for oxygen sensors and for catalytic reactors as membranes with oxygen-conducting properties [1-3], photocatalysts in UV and visible spectral regions [4, 5]. Bismuth niobate undergoes the reconstructive reversible phase transition from cubic phase to tetragonal one at 830 °C and the cubic phase appears again at 900 °C [6-8]. Cubic bismuth niobate is characterized by defective fluorite-like structure with the following parameters (*Fm3m*, $a = 0.548$ nm). Cation positions of bismuth (III) and niobium (V) are distributed in the same crystallographic system [9]. The niobium atoms are arranged in distorted coordination octahedra [6, 10], the niobium-oxygen octahedra are bound by oxygen vertices, forming chains or blocks [3, 6, 10-14]. Previous studies of the magnetic properties of solid solutions of niobate of bismuth of cubic modification containing paramagnetic ions of 3d-elements [15-17] have shown that, due to the charge imbalance and highly distorted coordination polyhedron in the dilute solutions, the paramagnetic atoms were preferably in the oxidized state, e.g. Ni(III), Mn(III), Mn(IV). The concentrated solid solutions Bi₃Nb_{1-x}M_xO_{7-δ} (M – Ni, Mn) are stabilized by the formation of clusters of paramagnetic atoms with the antiferromagnetic exchange type, which manifestation is possible due to aggregated niobium-oxygen octahedra in the structure.

In this paper, the state and nature of the iron paramagnetic exchange interactions in the Bi₃Nb_{1-x}Fe_xO_{7-δ} solid solutions were studied by means of magnetic dilution, EPR and NEXAFS-spectroscopy. The parameters of exchange interactions in clusters of iron atoms were calculated. The solid solution composition as a function of the content of paramagnetic atoms was modelled.

Experimental part

The samples of bismuth orthoniobate solid solutions of cubic modification were synthesized by the solid-phase method from “special pure” grade oxides of bismuth (III), niobium (V) and iron (III). This method included staged calcination at the temperatures of 650 °C and 950 °C. Phase composition of the samples was monitored by means of scanning electron microscopy (electron scanning microscope Tescan VEGA 3LMN, energy dispersion spectrometer INCA Energy 450) and X-ray phase analysis (a DRON-4-13 diffractometer, CuK α emission), parameters of the unit cell of the solid solutions were calculated using the CSD program package [18]. The quantitative measurement of iron content in the samples was performed by atom-emission spectrometry (a spectrometer SPECTRO CIROS of ICP type), the accuracy was $\pm 5\%$ of the parameter x in the formula of the solid solutions. In the study of the solid solution samples, the magnetic susceptibility was measured by the Faraday method at sixteen fixed temperatures in the temperature range of 77–320 K. The relative measurements were characterized by the accuracy of 2%. The spectra of EPR of the polycrystalline bismuth orthoniobate preparations were registered using a RadioPAN SE/X 2547 radiospectrometer of X-diapason (Center for Collective Usage “Geonauka” at the Institute of Geology of Komi Scientific Center of Ural Branch of RAS). Spectra were received at room temperature using a rectangular resonator (RX102, TE 102 mode) in the form of the first derivative at the 100 MHz HF modulation frequency with the 0.25 mT amplitude and the 35 mW SHF field power. A batch of a preparation (≈ 100 mg) was placed into a quartz tube with 4 mm external diameter. The anthracite EPR signal ($g_0 = 2.0032$, $B_{pp} = 0.5$ mT) was used for amplification calibration of the instrument. The spectra were recorded in the magnetic field range from 0 to 700 mT and the

lines of the reference were separately recorded with the scan step of 5 mT. The total spectra were normalized to the reference line intensity and then to 100 mg of the sample. The near-edge X-ray absorption fine structure (NEXAFS) of the Fe2p-absorption spectra of the iron-containing solid solutions Bi₃Nb_{1-x}Fe_xO_{7-δ} and oxides of iron was received using a synchrotron radiation source at the BESSY-II, Russian–German beamline in Berlin [19]. Each spectrum was registered in the mode of total electron yield (TEY) [20].

Results and discussion

The solid solutions Bi₃Nb_{1-x}Fe_xO_{7-δ} were obtained in the narrow concentration interval, $x \leq 0.06$ [21]. The measurements of magnetic susceptibility allowed us to calculate the paramagnetic components of the magnetic susceptibility for the solid solutions and the values of the effective magnetic moments of iron atoms corresponding to various concentrations of the solid solutions and temperatures. The diamagnetic corrections for calculating the paramagnetic component of the magnetic susceptibility were taken considering the susceptibility of the matrix of bismuth niobate Bi₃NbO₇ of cubic modification, measured in the analogous temperature range [22]. The temperature dependence of the reciprocal of the magnetic susceptibility paramagnetic component, which was calculated for a mole of atoms of the paramagnetic obeyed the Curie-Weiss law in the investigated temperature range for all iron-containing solid solutions. The isotherms of a paramagnetic component of iron magnetic susceptibility [$\chi^{para}(\text{Fe})$] in the solid solutions (Fig. 1) have the form characteristic of antiferromagnets. The effective values of magnetic moment of single iron atoms, that were calculated by extrapolation of the [$\chi^{para}(\text{Fe})$] values' concentration dependencies to the infinitely diluted solid solutions, decreased with increasing temperature from $\mu_{\text{eff}}(\text{Fe}) = 7.12$ MB (90 K) to 6.97 MB (320 K). This indicated the presence of ferromagnetic interactions between paramagnetic iron atoms. The value of the magnetic moment was much greater than the pure spin value of Fe(III) atoms ($\mu_{\text{eff}} = 5.92$ MB, term ${}^6A_{1g}$), Fe(II) ($\mu_{\text{eff}} \sim 4.9$ –5.7 MB, ${}^5T_{2g}$), which indicated the formation of ferromagnetically bound aggregates of Fe(III) atoms in the highly diluted solid solutions.

The ferromagnetic nature of the interaction in iron clusters remained up to $x \leq 0.006$. The nature of the temperature dependent change in the magnetic moment with increasing paramagnetic atom

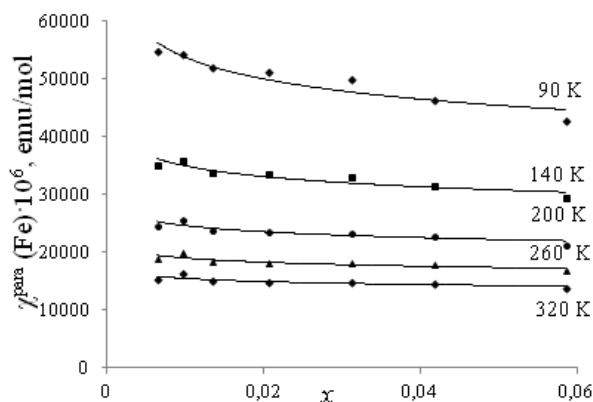


Fig. 1. Paramagnetic component isotherms of the magnetic susceptibility of the iron-containing preparations at 90–320 K

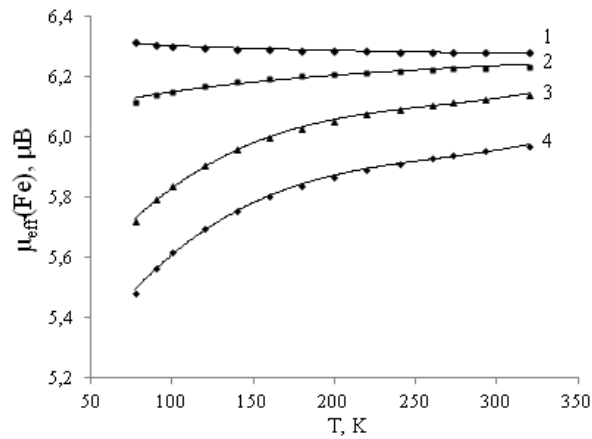


Fig. 2. Temperature dependencies of the effective magnetic moment of iron in the solid solutions at x 0.006 (1), 0.013 (2), 0.04 (3), 0.06 (4)

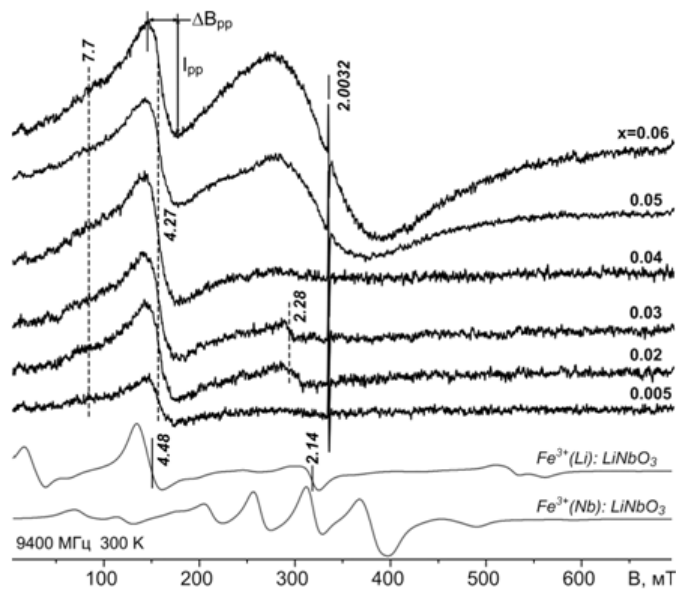


Fig. 3. EPR spectra of the samples of iron in the iron-doped Bi_3NbO_7 at various iron content x . The modelled powder spectrum of $\text{Fe}(\text{III})$ in positions of Li and Nb(V) in the LiNbO_3 lattice is below

concentration in the solid solutions indicated the dominance of the antiferromagnetic type of exchange between iron atoms (Fig. 2).

The spectra of EPR of the $\text{Bi}_3\text{Nb}_{1-x}\text{Fe}_x\text{O}_{7-\delta}$ solid solutions at $0.006 \leq x \leq 0.06$, as well as the calculated powder spectra of Fe^{3+} ions in cationic positions of lithium and niobium (V) of lithium niobate crystal with the parameters of the spin Hamiltonian of the Fe1 ($\text{Fe}^{3+}(\text{Li})$) and Fe4 ($\text{Fe}^{3+}(\text{Nb})$) centers are shown in Fig. 3 [21, 23, 24]. A software package Easyspin for the MathLab programming environment was used for the modeling of the spectra [25]. The narrow line on the experimental spectra with $g_0 = 2.0032$ refers to the standard.

The spectrum of the sample with minimum iron content contained a symmetric signal with $g = 4.27$ ($\Delta B_{pp} \approx 29$ mT) with a weak shoulder at $g \sim 8$. Such a spectrum can be explained by structurally isolated Fe³⁺ ions located in relatively strong crystal field, characterized by the parameter of axial field $D > h\nu_{SHF}$, where $\nu_{SHF} \sim 9.4$ MHz, and the maximum degree of orthorhombic distortion of $\sim 1/3$ [23]. Presumably, the appearance of the octahedral positions of iron with strong rhombic distortion is related with the compensation of excess charge by oxygen vacancies: Fe(III)→Nb(V) +V[O²⁻]. The V[O²⁻] vacancies in the nearest surroundings leads to the strong distortion of the octahedral position of iron and to the appearance of the band with 4.27 in the spectrum of EPR. The line with $g \sim 8$ can be associated with the presence of the paramagnetic atom aggregates [26].

The samples of Bi₃Nb_{1-x}Fe_xO_{7-δ} solid solutions at $0.02 \leq x \leq 0.04$ had a low-intensity broad band in the region of $g \sim 2.28$ of their spectra, which corresponds to iron (III) atoms occupying the cationic positions of bismuth, because a line with a close effective g-factor value is present in the spectrum of EPR of a resembling complex in monocystal niobate of lithium (Fig. 3). The low-field part of the broad line of 4.27 probably has a line of axial complexes of Fe (III)(Bi) with $g \sim 4.5$. The spectra of EPR of the solutions with $x > 0.04$ exhibited a broad, slightly asymmetric line ($\Delta B_{pp} \sim 100$ mT) centered around $g \sim 2.0$. The Lorentz shape approximated well the segment of the line in the high-field. The lack of noticeable structure of the line with g about 2.0 and the appearance of the signal in the high iron content samples indicated its origination from iron (III) ions in the octahedral coordination.

The solid solutions Bi₃Nb_{0.94}Fe_{0.06}O_{7-δ} as well as iron oxides FeO, Fe₂O₃ and Fe₃O₄ were studied by the NEXAFS spectroscopy in order to determine the degrees of oxidation of iron atoms. The analysis of the NEXAFS Fe2p-spectra of iron-containing solid solutions and iron oxides (Fig. 4) revealed that the studied Fe atoms were mainly in the +3 oxidation state. The spectra of iron oxides FeO recorded in the present study correspond to the Fe2p-spectra, which were studied earlier [20].

The solid solution compositions depending on the content of the paramagnetic were modeled by the theoretical estimation of the susceptibility and by the comparison of the calculated values with the experimentally obtained values.

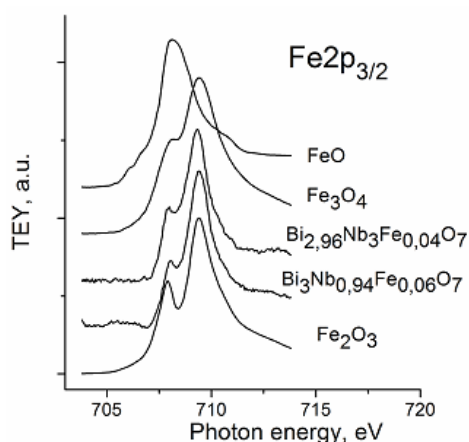


Fig. 4. NEXAFS Fe2p_{3/2}-spectra of the iron-doped Bi₃NbO₇ ceramics and iron oxides Fe₃O₄ and Fe₂O₃, FeO [20]

The computation and plotting of the experimental dependencies of $\chi^{para}(\text{Fe})$ on the solid solution concentrations were carried out within the framework of the dilute solid solution model, on the basis which, the magnetic susceptibility is defined as the sum of the contributions from paramagnetic atoms which are considered to be single (Fe(III), monomers) and their M-O-M aggregates bound by exchange (dimers, Fe(III)-O-Fe(III)). The equation for finding the paramagnetic component of the iron atom magnetic susceptibility is the sum of the contributions of the magnetic susceptibility of monomers, as well as the dimers with the anti- and ferromagnetic interactions:

$$\begin{aligned} \chi_{calc}^{para}(\text{Fe}) = & (1 - a_{\text{Fe(III)}}^{mon} - a_{\text{Fe(III)}}^{dim(a)}) \chi_{\text{Fe(III)-Fe(III)}}^{dim(f)} + \\ & + a_{\text{Fe(III)}}^{dim(a)} \chi_{\text{Fe(III)-Fe(III)}}^{dim(a)} + a_{\text{Fe(III)}}^{mon} \chi_{\text{Fe(III)}}^{mon}, \end{aligned} \quad (1)$$

where $a_{\text{Fe(III)}}^{mon}$ and $a_{\text{Fe(III)}}^{dim(a)}$ are the monomer fractions s and antiferromagnetically bound iron (III) dimers, $\chi_{\text{Fe(III)}}^{mon}$ is the Fe(III) monomer magnetic susceptibility $\chi_{\text{Fe(III)-Fe(III)}}^{dim(a)}$ and $\chi_{\text{Fe(III)-Fe(III)}}^{dim(f)}$ are the magnetic susceptibilities of the dimers (Fe(III)-O-Fe(III)) with ferro- and antiferromagnetic types of exchange, determined by the Heisenberg-Dirac-van Vleck model [27].

There are five independent parameters in the equation (1): the fractions of individual Fe(III) atoms and Fe(III)-O-Fe(III) dimers with an anti- and ferromagnetic exchange types, as well as the parameters of the anti- and ferromagnetic exchange between iron (III) atoms, $J_{\text{Fe(III)-Fe(III)}}$, which are indirectly present in this equation. As it was shown in several of works [15-19], the number of experimental magnetic susceptibility values as the function of the temperature and the solid solution concentration is sufficient to estimate the exchange parameter and the fraction of clusters of the atoms with paramagnetic properties.

According to the Heisenberg-Dirac-van Vleck model [27], Hamiltonian of the spin-spin interaction for a dimer looks like (2):

$$\hat{H}_{\text{exch}} = -2J\hat{S}_i\hat{S}_j. \quad (2)$$

Here, J is the parameter of isotropic exchange and S is the operator of the total angular spin moment.

Then χ_{dim} is determined with the help of the relationships (3) – (6).

$$\chi_{\text{dim}}^{S_1-S_2} = \frac{1}{2} \frac{\sum_{S'} g^2(S')S'(S'+1)(2S'+1)e^{-E(J,S')/kT}}{8T \sum_{S'} (2S'+1)e^{-E(J,S')/kT}}, \quad (3)$$

$$E(J, S') = -J[S'(S'+1) - S_a(S_a+1) - S_b(S_b+1)], \quad (4)$$

$$S' = S_a + S_b, S_a + S_b - 1, \dots, |S_a - S_b|, \quad (5)$$

where S_a, S_b are the values of spins of the atoms within the dimers, applying to this study, for the Fe(III)-O-Fe(III) dimer $S_a = S_b = 5/2$, g – the Lande factor for atoms of iron (III), J – the parameter of exchange, T – the absolute temperature.

The paramagnetic component of the magnetic susceptibility of Fe(III)-O-Fe(III) dimers was calculated by the equation (6):

$$\chi_{dim} = \frac{1}{4T} \cdot \frac{330e^{12.5x} + 180e^{2.5x} + 84e^{-5.5x} + 30e^{-11.5x} + 6e^{-15.5x}}{11e^{12.5x} + 9e^{2.5x} + 7e^{-5.5x} + 5e^{-11.5x} + 3e^{-15.5x} + e^{-17.5x}}, \quad (6)$$

where $x = J/kT$, where k – the Boltzmann constant.

The experimental and calculated values achieved the agreement via the reduction of the value of the function $\sum_i \sum_j (\chi_{ij}^{calc} - \chi_{ij}^{exp})^2$, where \sum_i is summation over all concentrations; \sum_j is summation over all temperatures; χ_{ij}^{calc} is the calculated value of paramagnetic component of the solid solution magnetic susceptibility, χ_{ij}^{exp} is the experimental paramagnetic component value. The best correlation between the experimental values and the calculated values was obtained for the iron-containing solid solutions with the antiferromagnetic exchange parameter $J_{Fe^{3+}-O-Fe^{3+}} = -180 \text{ cm}^{-1}$ and the ferromagnetic exchange parameter $J_{Fe^{3+}-O-Fe^{3+}} = 53 \text{ cm}^{-1}$. The comparison of the experimental and theoretical values of the magnetic susceptibility of the solid solutions is shown in Table 1.

It was established as a result that the solid solution with infinite dilution contains single atoms of Fe(III) and the dimers (Fe(III)-O-Fe(III)) with an antiferro- and ferromagnetic exchange types. As the solid solution iron concentration increased, the fractions of Fe(III) monomers and ferromagnetically bound dimers decrease along with the increase in the fractions of antiferromagnetically bound ones (Table 1). The change in the type of interaction among the atoms with paramagnetic properties in a cluster with increasing concentration can be explained by the degree of defectiveness of the oxygen surroundings and the nature of the distribution of atoms of iron over the cationic positions. It can be assumed that in the heterovalently-substituted solid solutions, the occurrence of the oxygen vacancies leads to the suppression of antiferromagnetic exchange channels of the type $d_{x^2-y^2} \parallel p_x \parallel d_{x^2-y^2}$ and to start the action of the ferromagnetic exchange channels $d_{x^2-y^2} \perp p_x \perp d_{xy}$. With an increase in the content of atoms of Fe(III) in these solutions, the fraction of exchange bound aggregates that stabilize the crystal structure are increasing due to the localization of aggregates near the oxygen vacancies, which reduces the degree of distortion of the oxygen surroundings of the paramagnetic atoms. This is the cause of the increase in the fraction of aggregates with antiferromagnetic exchange type, realized through the exchange channels $d_{x^2-y^2} \parallel p_x \parallel d_{x^2-y^2}$ and $d_{xz} \parallel p_z \parallel d_{xz}$. The appearance of the dimers

Table 1. The results of calculation of distribution of atoms of iron in the iron-doped Bi₃NbO₇¹

x	$a_{Fe(III)-Fe(III)}^{dim(f)}$	$a_{Fe(III)}^{mon}$	$a_{Fe(III)-Fe(III)}^{dim(a)}$	$\chi_{exp(calc)} \cdot 10^9, \text{ emu/mol}$				
				90 K	140 K	200 K	260 K	320 K
0.000	0.58	0.40	0.02	67.5(67.6)	43.6(43.6)	30.8(30.4)	24.0(23.2)	19.8(18.7)
0.006	0.42	0.34	0.24	56.2(56.1)	36.3(37.3)	25.3(26.4)	19.5(20.3)	15.9(15.9)
0.010	0.40	0.30	0.30	53.8(53.8)	35.1(36.2)	24.7(25.7)	19.0(19.8)	15.5(15.3)
0.013	0.39	0.28	0.33	52.0(52.6)	34.2(35.6)	24.2(25.3)	18.7(19.5)	15.3(15.0)
0.020	0.38	0.19	0.43	49.8(49.6)	33.1(34.1)	23.5(24.5)	18.3(18.9)	14.9(14.3)
0.031	0.36	0.15	0.49	47.6(47.2)	32.0(33.0)	22.9(23.8)	17.8(18.4)	14.6(13.8)
0.041	0.34	0.12	0.54	46.2(45.2)	31.3(31.9)	22.5(23.1)	17.6(17.9)	14.4(13.3)
0.059	0.32	0.10	0.58	44.6(45.4)	30.4(31.0)	22.0(22.5)	17.2(17.5)	14.2(12.9)

Footnote: $1 - a_{Fe(III)}^{mon}$ is a fraction of monomers of iron (III), $a_{Fe(III)-Fe(III)}^{dim(f)}$ is a fraction of dimers of iron (III) with ferromagnetic exchange, $a_{Fe(III)-Fe(III)}^{dim(a)}$ is a fraction of dimers of iron (III) with antiferromagnetic exchange.

instead of more complexly organized aggregates or paramagnetic atom chains is probably can be explained by the fact that these solid solutions have low concentration of the atoms with paramagnetic properties.

Conclusion

The measuring of the magnetic susceptibility, NEXAFS and EPR-spectroscopy of the iron-containing solid solutions of bismuth niobate Bi₃NbO₇ of cubic modification have indicated that iron atoms are represented by monomers of Fe(III) and exchange bound dimers with the antiferromagnetic type and ferromagnetic type of exchange. The parameters of the exchange in the dimers of atoms of iron (III) with an the anti- and ferromagnetic types of exchange, calculated according to the model of Heisenberg-Dirac-van Vleck, are equal to $J = -180 \text{ cm}^{-1}$ and $J = 53 \text{ cm}^{-1}$, respectively. The satisfactory convergence was observed between the calculated values of the magnetic susceptibility and the experimental values in the iron-doped Bi₃NbO₇ ceramics. The modeling of the solid solution compositions and nature of the exchange interactions in clusters allowed us to establish that the increasing solid solution content of the atoms with paramagnetic properties causes the increase in the fraction of dimers of Fe(III) atoms with antiferromagnetic exchange type. Along with it, the fractions of the monomers of Fe(III) and dimers with ferromagnetic type of exchange decrease.

References

1. Takahashi T., Iwahara H., Esaka T. Conduction in Bi₂O₃-based oxide ion conductor under low oxygen pressure. II. Determination of the partial electronic conductivity 1977. *J. Appl. Electrochem.* Vol. 7, P. 303-308.
2. Fung K.Z., Chen J., Virkar A.V. Effect of Aliovalent Dopants on the Kinetics of Phase Transformation and Ordering in RE₂O₃-Bi₂O₃ (RE = Yb, Er, Y, or Dy) Solid Solutions 1993. *J. Am. Ceram. Soc.* Vol. 76, P. 2403-2418.
3. Struzik M., Liu X., Abrahams I. et al. Defect structure and electrical conductivity in the pseudo-binary system Bi₃TaO₇-Bi₃NbO₇ 2012. *Sol. St. Ion.* Vol. 218, P. 25-30.
4. Fang J., Ma J., Sun Y. et al. Synthesis of Bi₃NbO₇ nanoparticles with a hollow structure and their photocatalytic activity under visible light 2011. *Sol. St. Scien.* Vol. 13, P. 1649-1653.
5. Wu W., Liang S., Shen L., Ding Z., Zheng H., Su W., Wu L. Preparation, characterization and enhanced visible light photocatalytic activities of polyaniline/Bi₃NbO₇ nanocomposites 2012. *J. Alloy. Compd.* Vol. 520, P. 213-219.
6. Zhou W., Jefferson D.A., Thomas J.M. A New Structure Type in the Bi₂O₃-Nb₂O₅ System 1987. *Sol. St. Chem.* Vol. 70, P. 129-136.
7. Zhuk N.A., Rozhkina N.V. VIII Phase Transitions and Electrophysical Properties of Bismuth Niobate 2014. *Russ. J. Gen. Chem.* Vol. 84, P. 3-7.
8. Ling C.D., Johnson M. Modelling, refinement and analysis of the “Type III” d-Bi₂O₃-related superstructure in the Bi₂O₃-Nb₂O₅ system 2004. *J. Sol. St. Chem.* Vol. 177, P. 1838-1846.
9. Castro A., Aguado E., Rojo J.M. et al. The new oxygen-deficient fluorite Bi₃NbO₇: synthesis, electrical behavior and structural approach 1998. *Mat. Res. Bull.* Vol. 33, P. 31-41.
10. Tang D., Zhou W. An Electron Diffraction Study of the Type II Bi_{2-x}Nb_xO_{3+x} Solid Solution 1995. *J. Sol. St. Chem.* Vol. 119, P. 311-318.

11. Abrahams I., Krok F., Wrobel W. et al. Defect structure in $\text{Bi}_3\text{Nb}_{1-x}\text{Zr}_x\text{O}_{7-x/2}$ 2008. *Sol. St. Ion.* Vol. 179, P. 2-8.
12. Abrahams I., Krok F., Kozanecka-Szmigiel A. et al. Effects of ageing on defect structure in the Bi_3NbO_7 - Bi_3YO_6 system 2007. *J. Pow. Sour.* Vol. 173, P. 788-794.
13. Abrahams I., Krok F., Chan S.C.M. et al. Defect structure and ionic conductivity in $\text{Bi}_3\text{Nb}_{0.8}\text{W}_{0.2}\text{O}_{7.1}$ 2006. *J. Sol. Electrochem.* Vol. 10, P. 569-574.
14. Leszczynska M., Holdynski M., Krok F. et al. Structural and electrical properties of $\text{Bi}_3\text{Nb}_{1-x}\text{Er}_x\text{O}_{7-x}$ 2010. *Sol. St. Ion.* Vol. 181, P. 796-811.
15. Chezhina N.V., Zhuk N.A. XII Magnetic Behavior of $\text{Bi}_3\text{Nb}_{1-x}\text{Mn}_x\text{O}_{7-\delta}$ Solid Solutions 2015. *Russ. J. Gen. Chem.* Vol. 85, P. 1777-1785.
16. Chezhina N.V., Zhuk N.A., Zharenkova V.N. et al. State of Nickel in $\text{Bi}_3\text{Nb}_{1-x}\text{Ni}_x\text{O}_{7-\delta}$ Solid Solutions with a Fluorite-Type Structure 2015. *Russ. J. Gen. Chem.* Vol. 85, P. 353-358.
17. Chezhina N.V., Zhuk N.A., Korolev D.A. The exchange interactions and the state of manganese atoms in the solid solutions in Bi_3NbO_7 of cubic and tetragonal modifications 2016. *J. Sol. St. Chem.* Vol. 233, P. 205-210.
18. Akselrud L.G., Gryn Yu.N., Zavalij P.Yu. et al. *CSD-universal program package for single crystal or powder structure data treatment* 1985. Thes. Rep. XII Eur. Crystallogr. Meet. P.155.
19. Stöhr J. *NEXAFS Spectroscopy*. Springer, Berlin.1992.
20. Regan T.J., Ohldag H., Stamm C. et al. Chemical effects at metal/oxide interfaces studied by x-ray-absorption spectroscopy 2001. *Phys. Rev. B.* Vol. 64, P. 214422.
21. Chezhina N.V., Korolev D.A., Zhuk N.A. et al. Exchange interactions and the state of iron atoms in $\text{Bi}_3\text{Nb}_{1-x}\text{Fe}_x\text{O}_{7-\delta}$ 2017. *J. Sol. St. Chem.* Vol. 247, P. 8-12.
22. Chezhina N.V., Zhuk N.A., Lyutov V.P. IX Magnetic Susceptibility of Bi_3NbO_7 of Cubic and Tetragonal Modifications 2015. *Russ. J. Gen. Chem.* Vol. 85, P. 1073-1075.
23. Malovichkov G.I., Grachev V.G., Schirmer O.F. et al. New axial Fe^{3+} centres in stoichiometric lithium niobate crystals 1993. *J. Phys. Condens. Matt.* Vol. 23, P. 3971-3976.
24. Razdobarin A.G., Basun S. A., Bursian V.É. et al. A $\text{Fe}[\text{Nb}]\text{-Li}$ Center in Stoichiometric LiNbO_3 Crystals: Mechanism of Formation 2010. *Phys. Sol. St.* Vol. 52, P. 706-711.
25. Stoll S., Schweiger A. EasySpin, a comprehensive software package for spectral simulation and analysis in EPR 2006. *J. Magn. Reson.* Vol. 178, P. 42-55.
26. Lou V. *Paramagnetic resonance in solids*. Nauka, Moscow, 1962.
27. Rakitin Yu.V. *Introduction to Magnetochemistry*. Method of Static Magnetic Susceptibility in Chemistry. Nauka, Moscow, 1980.